SINERGI Vol. 30, No. 1, February 2026: 23-30
http://publikasi.mercubuana.ac.id/index.php/sinergi
http://doi.org/10.22441/sinergi.2026.1.003

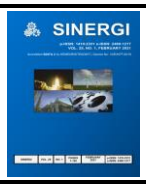

Compound development as a protective layer on FeCrAl substrate by a combination of γ-Al_2O_3 ultrasonic and NiO electroplating techniques to improve thermal stability

Imam Hidayat[1], Dafit Feriyanto[1]*, Supaat Zakaria[2], SS. Abdulmalik[3], Nurato Nurato[1], Dedik Romahadi[1]
[1]Department of Mechanical Engineering, Faculty of Engineering, Universitas Mercu Buana, Indonesia
[2]Department of Mechanical Engineering, Politeknik Ungku Omar, Malaysia
[3]Department of Mechanical Engineering, Nigerian Army University, Nigeria

Abstract
One of the most technologically advanced methods for developing and adhering catalysts to the FeCrAl substrate is electrophoretic deposition. However, it faces a problem: low thermal stability at high temperatures of 10000 °C, caused by a lack of a protective oxide layer. The goal of this study is to investigate the protective oxide layers formed by Al_2O^3 and NiO coatings on FeCrAl metallic material for catalytic converters (CATCO). The electrolyte was prepared with distilled water at a constant temperature of 40±50 °C. The pH was adjusted to 5 with HCl and NaOH reagents. The electrolyte was prepared at 40 ± 50 °C and stirred for 1 minute using a magnetic stirrer. A 50mm x 10mm Ni plate substrate served as the anode, while a 40mm x 20mm FeCrAl cathode was used. The spacing between the anode and cathode was set at 25mm. The electroplating was conducted for several variation times of 15, 30, 45, 60 and 75 minutes, current density of 8 A/dm2, 3g γ-Al_2O_3 was inserted into the beaker for each sample and the total surface area was 1600mm^2 on both sides. Drying was performed after electroplating at 600 °C for 12 hours. Raman spectroscopy revealed that several compounds observed during the experimental stages, such as FeCrAl, γ-Al2O3, NiO, NaO_2, $NiAl_2O_4$, $NiCr_2O_4$, and $FeCr_2O_3$, were also present in the coated FeCrAl CATCO, with distinct peaks. Therefore, it can be concluded that the UB+EL 30 min successfully deposited the γ-Al_2O_3 and NiO on the FeCrAl substrate after CATCO fabrication.

Keywords:
Catalytic converter;
Electroplating;
FeCrAl;
Oxide layer;
Thermal stability;

Article History:
Received: August 3, 2024
Revised: December 22, 2024
Accepted: June 14, 2025
Published: January 2, 2026

Corresponding Author:
Dafit Feriyanto
Mechanical Engineering Department, Universitas Mercu Buana, Indonesia
Email: imam.hidayat@mercubuana.ac.id

INTRODUCTION

Exhaust technology had been a major focus among researchers, and it had been used by automotive manufacturers all over the world [1][2]. There are three (3) principal pollutants in the exhaust emission system of a gasoline engine: carbon monoxide (CO), nitrogen oxides (NOx), and hydrocarbon (HC) as unburned components. These pollutants were high in the atmosphere because the CATCO components in the exhaust emission system were inefficient at reducing exhaust gas emissions. To fulfil strength standard, the Catalytic converter (CATCO) is redesigned and investigated using simulation, material, and method selection to characterize the monolith substrate and optimize the CATCO [3]. A common CATCO design was the Three Way Catalytic (TWC) converter, which conducts reduction-oxidation simultaneously.

There are three key components of CATCO: washcoat material, substrate, and catalyst. Currently, metallic CATCO was an

interesting component to investigate in comparison to ceramic material. As a result, the predominant CATCO component in this investigation was the FeCrAl metallic substrate. FeCrAl is commonly referred to as metallic substrates due to their great thermal stability and corrosion resistance, as well as the strong adherence of oxide film to the substrate's surface when the suitable surface treatment is done [4, 5, 6, 7, 8]. Excellent oxidation catalyst materials have often been based on precious metals. However, these materials are expensive, in short supply [8, 9, 10], have a high specific activity, are easily oxidized, and break easily at temperatures ranging from 500 to 900^{0}C [11].

Catalyst layers on metallic surfaces are emerging as one of the most important coating technologies for producing structures like metallic honeycombs and micro reactors. Pressure drop, heat and mechanical resistance are frequently important concerns in catalytic reactors, and metallic honeycombs (monoliths) are an effective solution under extreme settings, such as automotive catalyst converters with cold start and exhaust velocity fluctuation [9][12].

Recently, mesoporous Ni-Al oxide was synthesized using a one-pot synthesis, resulting in a high BET surface area of 385m^2/g and increased thermal stability. High BET surface area for mesoporous Ni-Al is in range of 350-409 m^2/g [6]. The related oxides were originally used to partially oxidize methane into synthesis gas at ambient pressure. It was observed that a rather strong contact between the nickel species and alumina substrate resulted in finely dispersed nickel particles on the catalyst surface, which prevented coke formation [1,13,14].

According to [15, 16, 17] that the most popular method for developing an oxide coating layer on a metallic substrate is dip coating. Before applying the washcoat, it is paired with a shorter diffusion route [17]. The FeCrAl alloy is prepared by the other researchers via sol-gel, spray-pyrolysis, and co-precipitation techniques [4]. In addition, the FeCrAl substrate is developed and bound to the catalyst through the use of in-situ hydrothermal [7], ultrasonic [18, 19, 20, –21], magnetron sputtering [22], and on-step hybrid deposition [23]. That approach is limited, though, in cases where NiO does not penetrate straight to the substrate. Therefore, this research is purposed to penetrate the NiO and γ-Al_2O_3 on FeCrAl in order to develop compound as protective layer that believe give a significant improvement on the thermal stability.

METHOD

Ultrasonic bath is conducted to FeCrAl foil that cuted in size of 40 mm x 20 mm and coating material is γ-Al_2O_3 powder. The samples are submerged in ethanol for five minutes. A frequency of 35 kHz and different ultrasonic times of 1, 1.5, 2, 2.5, and 3 hours are enforced during the ultrasonic process. The samples are submerged in a beaker containing 3 g of γ-Al_2O_3 powder per sample and 20 g/l of ethanol as shown in Figure 1. The next step is drying, which is done for 12 hours in an oven set at 60^{0}C.

Electrolyte, anti-pitting agent, anode, and cathode are some of the components used in the electroplating process as shown in Figure 2. The electrolyte medium utilized was sulphamate type, which is composed of sodium dodecyl sulphate ($C_{12}H_{25}OSO_3$.Na), boric acid (H_3BO_3), nickel (ii) chloride ($NiCl_2 \cdot 6H_2O$), and nickel (ii) sulphate 6-hydrate ($NiSO_4.6H_2O$). Table 1. shows the composition of this mixture. The electrolyte was made with distilled water and kept at a steady 40 to 50^{0}C. The pH of the solution was then brought to 5 with the help of HCl and NaOH reagent. With a magnetic stirrer, the electrolyte was stirred. A 50 mm × 10 mm nickel (Ni) plate substrate served as the anode, and a 40 mm x 20 mm FeCrAl served as the cathode. The adjustment was made to the anode and cathode distance at 25 mm. Electroplating was done for 15, 30, 45, 60, and 75 minutes with an 8 A/dm^2 current density, 3 g γ-Al_2O_3 in the beaker, and a total surface area of 1600 mm^2 on both sides. Following the electroplating process, a 12-hour drying process was carried out at 60^{0}C.

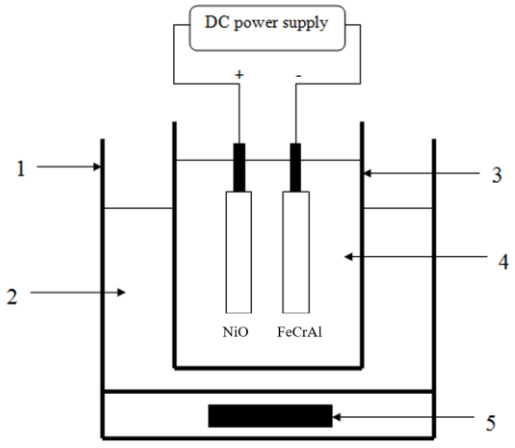

Figure 1. Schematic diagram of ultrasonic bath during electroplating; (1) Ultrasonic bath tank; (2) water; (3) biker; (4) sulphamate type electrolyte and (5) ultrasonic source

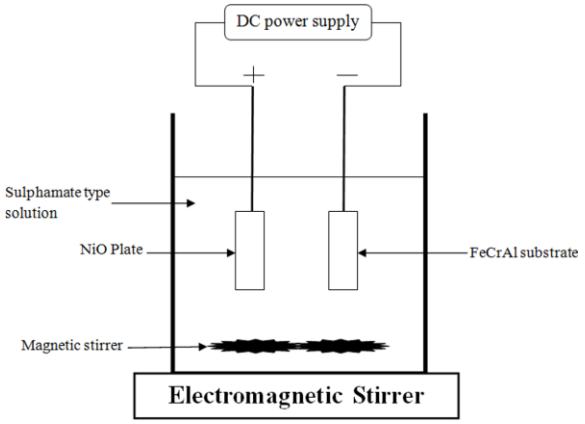

Figure 2. Schematic diagram of electroplating process

Table 1. Chemical composition of electrolyte

Electrolyte solution	Composition (%)
$NiSO_4.6H_2O$	51.25
$NiCl\ 6H_2O$	0.85
H_2BO_3	5.12
$C_{12}H_{25}SO_4Na$	42.73

The Raman spectroscopy machine (HORIBA Xplora Plus Raman Microscope) was used under environmental conditions. The materials used in this test were Coated FeCrAl CATCO by UB+EL 30 minutes, which had been produced and coated. According to [24] that the UB+EL 30 minutes has the best coating structure, fully embedded coating material on substrate than other parameters. The testing material had dimensions of 10 x 10mm (LxW), a thickness of 0.13mm, and a sinusoidal wave surface on the coated FeCrAl substrate. The goal is to ensure that washcoat material is deposited in all areas of the FeCrAl substrate. This testing was conducted at magnification of 50 times, laser strength of 1064/532 nm, slit 100 μm, accumulation of 2, and grating of 1200 (500 nm) as well as source of spectrum is from HORIBA scientific. Before Raman spectroscopy selected, the evaluation has been conducted to other testing and the result not as complete as Raman Spectroscopy.

RESULTS AND DISCUSSION

XRD testing of UB samples

Figure 3 displays the XRD study of FeCrAl substrate coated with γ-Al_2O_3 using ultrasonic method with holding times of 1, 1.5, 2, 2.5, and 3 hours. Major compounds found in UB samples include FeCrAl, FeO, γ-Al_2O_3, and $FeCr_2O_3$. The presence of FeCrAl and γ-Al_2O_3 in these samples indicates that the ultrasonic bath approach did not result in phase transition.

Broader peaks on strong line peaks are observed at the maximum of UB 1.5 h and gradually sharpen up to ultrasonic time of 3 h, indicating that UB 1.5 h has the lowest crystallite size when compared to other UB samples. However, in UB 2 h, low diffraction peaks occur due to displacement inaccuracy and the sample is located below the diffractometer's focal plane.

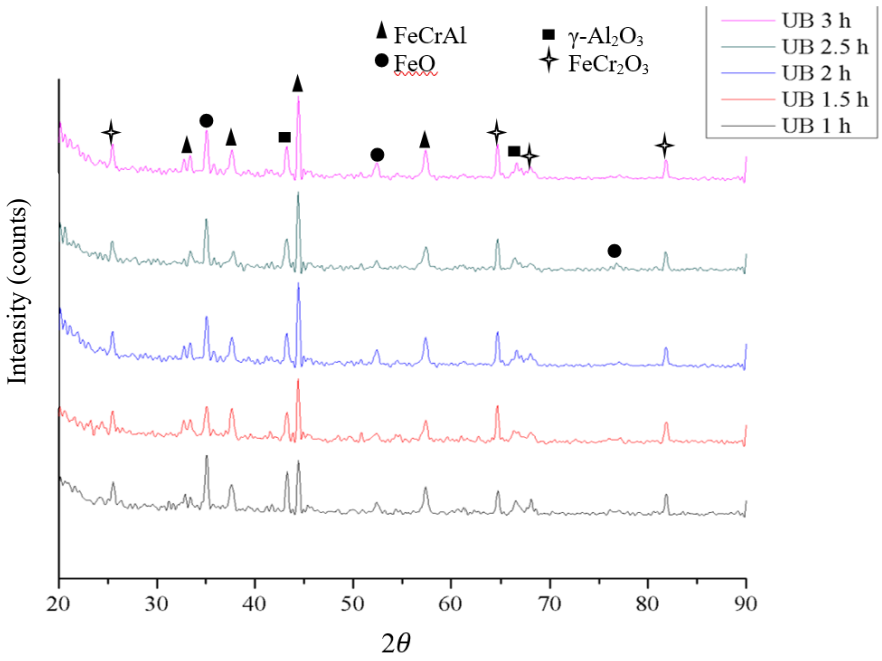

Figure 3. XRD peaks of UB samples

The association between compound analysis and thermal stability and conductivity study revealed that the UB sample has a lower mass change of 17.46 mg and a greater conductivity of 2.80E-04 S/cm when compared to the raw material of 23.39 mg and 4.65E-05 S/cm, respectively. In UB samples, a few compounds produced via the UB process were found to boost thermal stability at 1000^0C as well as material conductivity.

Microstructure investigation confirms γ-Al_2O_3 deposition on FeCrAl substrate, revealing embedded particles. The association between chemical analysis and cross section analysis of UB samples reveals a coating layer that protects the substrate material from high temperature operation and harsh conditions in the exhaust emission system. Coating thickness study confirms that UB samples had the highest coating thickness of 2.8 µm, while raw material has no coating thickness since no coating process was undertaken. The thickness data was automatically measured by XRD machine and it validated in other result that has been published [24]

XRD testing of UB+EL samples

The UB+EL approach was used to boost compound development and coating thickness of substrate material because it involves two deposition processes. The first deposition was done using the UB approach, with ethanol as the electrolyte and γ-Al_2O_3 as the coating material. The second deposition was carried out using the EL approach with a sulphamate solution as an NiO as the anode and FeCrAl as the cathode. Compound analysis of UB+EL samples, as illustrated in Figure 4.

UB+EL samples have yielded numerous compounds, including FeCrAl, FeO, γ-Al_2O_3, $FeCr_2O_3$, NiO, NaO_2, $NiAl_2O_4$, and $NiCr_2O_4$. FeCrAl contains γ-Al_2O_3. That compound was fully examined in UB+EL for 30 minutes, and significant diffraction peaks were found. Diffraction peaks widened with increasing UB+EL duration, indicating that γ-Al_2O_3 causes plastic deformation. Microstructure investigation confirmed that increased particle embedding leads to longer UB+EL holding times. In the lower UB+EL holding time, the lower particle is embedded on the FeCrAl substrate.

Fe-based alloys and Ni-based alloys have been found in high concentrations on coated FeCrAl substrates. These alloys are highly thermally stable at temperatures as high as 1400^0C. The coating substance formed a protective oxide layer, which was used to shield FeCrAl CATCO from the harsh conditions of the exhaust emission system. This was approved by [16][19], who stated that the coating material was used as a media for catalyst activation to develop a protective oxide layer. [3] also stated that Ni electroplating is performed for finishing technology, which is commonly used in the automobile industry. As a result, the combination of two processes has proven an intriguing way to manufacture FeCrAl CATCO.

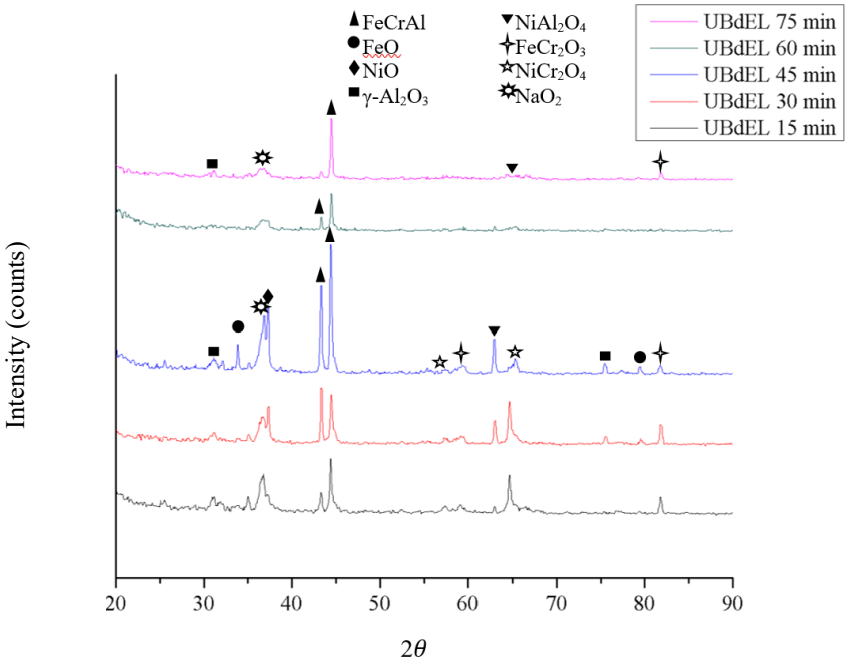

Figure 4. XRD peaks of UB+EL samples

An appropriate chemical concentration seen in UB+EL samples lead to the UB+EL sample's higher thermal stability, with a mass change of 2.85 mg when compared to UB and UBdEL samples. The coating material and catalyst were embedded on the FeCrAl substrate in the UB+EL samples, as confirmed by cross section analysis and coating thickness analysis. The UB+EL samples had the highest coating thickness of 13 µm when compared to UB, UBdEL, and EL. This result suggests that the UB+EL approach was effective in increasing thermal stability by increasing the protective oxide layer on the FeCrAl substrate, as seen by the increased coating thickness.

XRD testing of EL samples

Figure 5 shows the XRD examination of a FeCrAl substrate covered with an electroplating process for 15, 30, 45, 60, and 75 minutes. The three strongest diffraction peaks are situated at dispersed angles 2θ of 37.10, 44.70, 63.70, and 65.50. Na is present in these samples because it is incorporated into the electrolyte solution, which is a sulphamate solution. This solution is utilized with specific compositions such as 51.25% $NiSO_4.6H_2O$, 0.85% $NiCl\ 6H_2O$, 5.12% H_2BO_3, and 42.73% $C_{12}H_{25}SO_4$ Na. As a result, significant Ni and Na concentrations were found in EL samples.

Boric Acid (H_2BO_3) is used as a Process Control Agent (PCA) in sulphamate types to prevent agglomeration of solid forms (γ-Al_2O_3 powder). It acts as an absorber on particles with low surface tension. PCA can reduce γ-Al_2O_3 particle size by 2-3 times compared to its initial size. It supported by previous study that the particle size is significantly decrease by minimizing the agglomeration [24, 25, 26]

Several compounds appear on all diffraction peaks, including FeCrAl, FeO, γ-Al_2O_3, $FeCr_2O_3$, NiO, $NiAlO_4$, $NiCr_2O_4$, and NaO_2. Strong line peaks for FeCrAl and γ-Al_2O_3 indicate that no phase transition occurred during electroplating. Those chemicals were seen in EL 30 minutes to create a material with improved heat stability [14].

The thermal stability of EL samples is influenced by compound formation throughout the coating process. The data shows that EL samples had a higher thermal stability of 3.99µm than raw material, UB, and UBdEL samples. Higher thermal stability is achieved by combining NiO with electrolyte solution, which increases compound formation during the process.

NiO and γ-Al_2O_3 powder embedded on FeCrAl substrate resulted in increased surface roughness of 0.69 µm in EL samples compared to raw material and UB samples, indicating improved bonding activity. Cross-sectional examination confirms stronger bonding between NiO and γ-Al_2O_3 powder, revealing a coating layer following Ni-electroplating. Coating thickness study revealed that EL samples had a higher coating thickness of 11.3 µm compared to raw material, UB, and UBdEL samples.

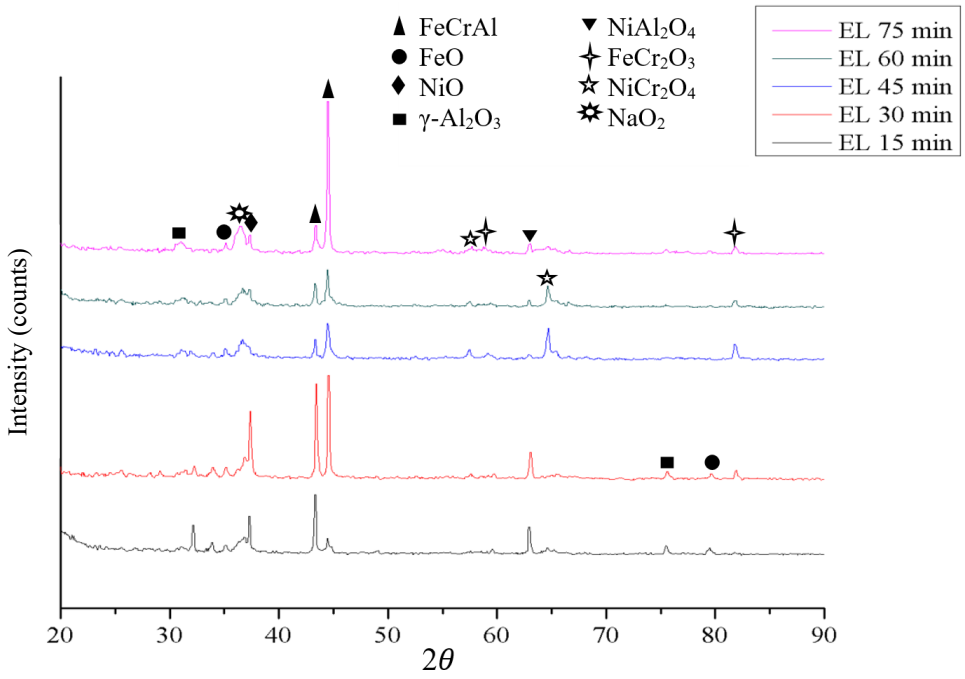

Figure 5. XRD peaks of EL samples

Raman spectroscopy testing

In Raman spectroscopy analysis, there are 5 samples from Coated FeCrAl CATCO which has been fabricated in sinusoidal wave. The samples selected from different location of FeCrAl CATCO which is 2 samples from side position and 3 samples from middle position which purposed to prove that coating activity of γ-Al_2O_3 and NiO on FeCrAl CATCO has been successfully embedded. Raman spectrum of side position was shown in Figure 6. Meanwhile for Raman spectrum of middle position was shown in Figure 7.

Raman Spectrum is a plot of intensity of Raman scattered radiation as a function of its frequency differences from the incident radiation where that differences were called by wave number. Raman spectrum of this samples was consists of 4 strong peaks that shows by wave number of 550-580 cm^{-1}, 700-750 cm^{-1}, 1100-1500 cm^{-1} and 200-300 cm^{-1}. Raman spectrum of coated FeCrAl CATCO mainly consists of FeCrAl, NaO_2, $FeCr_2O_3$, $NiAl_2O_4$, $NiCr_2O_3$ and γ-Al_2O_3. The highest spectrum of side position at 733cm^{-1} and 742cm^{-1} that consists of $FeCr_2O_3$ compound. In lower wave number which consists of NaO_2 at 577.133cm^{-1} and 566.169cm^{-1} as well as FeCrAl at 226.258cm^{-1}.

Figure 6 shows that $NiAl_2O_4$ and γ-Al_2O_3 at 1438.388cm^{-1} and 2918.892cm^{-1}, respectively. High intensity of side position of coated FeCrAl CATCO caused by high coating activity that occurred during UB+EL coating process. Therefore, Ni, Na and γ-Al_2O_3 strongly observed in these spectrums. Cr_2O_3 scale which combined with Fe and Ni promote the increment thermal stability at high temperature up to 1000^{0}C [26]. The compound that observed in XRD and Raman Spectroscopy testing is potentially improve thermal stability as stated in previous research [24][26].

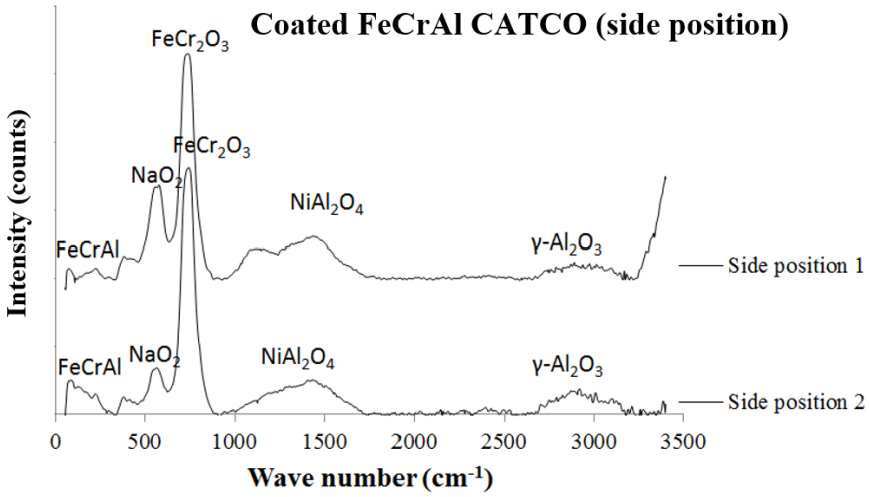

Figure 6. Raman spectrum of Coated FeCrAl CATCO (side position)

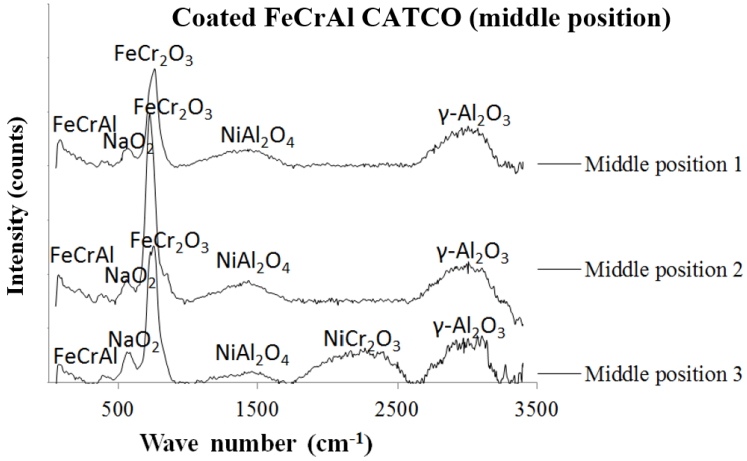

Figure 7. Raman spectrum of Coated FeCrAl CATCO (middle position)

The Raman spectrum of coated FeCrAl CATCO in middle position are shown in Figure 7 that mainly consists of 4 strong peaks which observed several compounds such as $FeCr_2O_3$ in strongest peaks, NaO_2 in wave number of 553.186 cm^{-1}, 562.174cm^{-1} and 517.139cm^{-1}, FeCrAl observed at 395.864cm^{-1} and 380.582cm^{-1}. Moreover, $NiAl_2O_4$ compound also observed at range of 1226 to 1490 cm^{-1}, $NiCr_2O_3$ at 2077 to 2200 cm^{-1} as well as γ-Al_2O_3 observed at the last peaks of 3006.164 cm^{-1}.

CONCLUSION

Metallic FeCrAl catalytic converter without coating shows the weakness regarding on thermal stability that caused by minimum protective oxide layer and to improve it, the FeCrAl catalytic converter is produced and coated using the proper procedure and parameter, UB+EL 30 minute. The prototype has dimensions of 65 x 125 mm (length x diameter). To ensure the deposition of washcoat material, Raman spectroscopy studies were done to analyze compound development following the production and coating processes. Raman spectroscopy examination revealed the presence of FeCrAl, γ-Al_2O_3, NiO, NaO_2, $NiAl_2O_4$, $NiCr_2O_4$, and $FeCr_2O_3$ in coated FeCrAl CATCO with significant peaks. After CATCO manufacturing, UB+EL for 30 minutes successfully deposited γ-Al_2O_3 and NiO on FeCrAl substrate.

ACKNOWLEDGMENT

The authors would like to express thanks to Universitas Mercu Buana for funding and facilities support while research conducted.

REFERENCES

[1] J. Huang et al., "Early-in-life inhalation exposure to diesel exhaust enhanced high fat diet-induced atherosclerosis via CD36-NLRP3 inflammasome / TXNIP," *Ecotoxicology and Environmental Safety,* vol. 306, p. 119356, 2025, doi: 10.1016/j.ecoenv.2025.119356

[2] A. Youssef, and A. Ibrahim, "NOx emissions reduction through applying the exhaust gas recirculation (EGR) technique for a diesel engine fueled with a diesel-biodiesel-diethyl ether blend," *Energy Storage and Saving*, vol. 3, pp. 318–326, 2024, doi: 10.1016/j.enss.2024.10.003

[3] S. Apaydin, and N. Doner, "Flow analysis in different geometries for optimization of exhaust manifold in a Locomotive diesel engine," *Ain Shams Engineering Journal*, vol. 15, p. 102974, 2024, doi: 10.1016/j.asej.2024.102974

[4] H. Pranoto, D. Feriyanto, and S. Zakaria, "Performance and Exhaust Gas Temperature Investigation of Ceramic, Metallic and FeCrAl Catalytic Converter in Gasoline Engine," *SINERGI*, vol. 23, no. 1, pp. 11-16, 2019, doi: 10.22441/sinergi.2019.1.002

[5] H. Pranoto, N. Nurato, and D. Feriyanto, "Coating Thickness Analysis of Deposited FeCrAl Substrate by Γ-Al2o3 Through Nio-Electroplating," *SINERGI*, vol. 22, no.3, pp. 177-184, 2018, doi: 10.22441/sinergi.2018.3.006

[6] G. Santosh, Kumar, S. Badulla, J. N. P. H. J. Venkatesh, G. Narasimhulu, and V. S. Rao, "Design and analysis of 3-way catalytic converter using CFD," *Materials today: Proceedings*, vol. 115, pp. 193-198, 2024, doi: 10.1016/j.matpr.2023.07.215

[7] Z. M. A. Ahmed et al., , "Recovery of tungsten from catalytic converter scraps using a Schiff-base adsorbent and subsequent preparation of tungsten oxide nanoparticles," *Materials Chemistry and Physics*, vol. 344, p. 131146, 2025, doi: 10.1016/j.matchemphys.2025.131146

[8] T. Cao et al., "La-doped macroporous carbon fiber catalytic converter for tetracycline efficient removal," *Chemical Engineering Journal*, vol. 480, p. 148075, 2024, doi: 10.1016/j.cej.2023.148075

[9] Y. Yu, J. Guo, G. Zhang, M. Wang, and J. Wang, "Rare earth metal modified CaO catalysts Ln/CaO (Ln=La, Ce, Nd) for oxidative coupling methane: Revealing the interaction between metal oxide and carrier," *Molecular Catalysis*, vol. 578, p. 115014, 2025, doi: 10.1016/j.mcat.2025.115014

[10] Z. Xu, R. Chen, Z. Mao, B. Wang, Z. Zhao, Y. Zhang, M. Cui, Y. Hou, C. Han, J. Yang, and X. Huang, "Enhancing NO oxidation performance through rare earth element-mediated modulation of Mn d-Band centers in Ce-Me-Mn mixed oxides," *Journal of Catalysis*, vol. 453, p. 116530, 2026, doi: 10.1016/j.jcat.2025.116530

[11] Y. Tan, E. Jiaqiang , C. Kou, C. Feng, and D. Han, "Effects of critical structure parameters on conversion performance enhancement of a Pd–Rh dual-carrier catalytic converter for heavy-duty natural gas engines," *Energy,* vol. 303, p. 131934, 2024, doi: 10.1016/j.energy.2024.131934

[12] K. D. Patel, D. Subedar, and F. Patel, "Design and development of automotive catalytic converter using non-nobel catalyst for the reduction of exhaust emission: A review," *Materials today: Proceedings*, vol. 57, pp.

2465-2472, 2022, doi: 10.1016/j.matpr.2022.03.350
[13] I. Chidunchi, M. Kulikov, R. Safarov, and E. Kopishev, “Extraction of platinum group metals from catalytic converters,” *Heliyon*, vol. 10, p. e25283, 2024, doi: 10.1016/j.heliyon.2024.e25283
[14] D. Pai, and M. K. Prabhu, “Recent Advances in Substrate Materials and Thermal Analysis of Catalytic Converters,” *Materials today: Proceedings*, vol. 5, no. 11, pp. 24221-24230, 2018, doi: 10.1016/j.matpr.2018.10.217
[15] D. Yang, Q. Yang, W. Ma, X. Ma, S. Wang, Y. Lei, “Characteristics of spent automotive catalytic converters and their effects on recycling platinum-group-metals and rare-earth-elements,” *Separation and Purification Technology*, vol. 308, p. 122977, 2023, doi: 10.1016/j.seppur.2022.122977
[16] G. S. Sharma, M. Sugavaneswaran, and R. Prakash, “Design and validation of additive manufactured catalytic converter for the control of regulated and unregulated emissions of a gasohol fuelled spark ignition engine,” *Fuel*, vol. 309, p. 122146, 2022, doi: 10.1016/j.fuel.2021.122146
[17] M. H. Morcali, “A new approach to recover platinum-group metals from spent catalytic converters via iron matte,” *Resources, Conservation and Recycling*, vol. 159, p. 104891, 2020, doi: 10.1016/j.resconrec.2020.104891
[18] Z. Zhou, and C. Chen, “A New Combined Method to Enhance Adhesive Bonding of Al_2O_3 Ceramic/Aluminum by Chemical Pretreatment and Ultrasonic,” *Chinese Journal of Mechanical Engineering*, p. 100133, 2025, doi: 10.1016/j.cjme.2025.100133
[19] H. Chen, F. Yang, Z. He, L. Huang, Y. Zhao, C. Dai, R. He, and H. Ma, “Influence of in situ 20 ± 2/28 ± 2 kHz dual-frequency ultrasonication on enzymolysis kinetics, thermodynamics and antioxidant activity of housefly (*Musca Domestica*) larvae protein hydrolysate,” *Ultrasonics Sonochemistry*, vol. 122, p. 107599, 2025, doi: 10.1016/j.ultsonch.2025.107599
[20] L. Ningqing , W. Rongshan, G. Ruonan , W. Linlin, H. Zhang, G. Changsheng, and X. Jian, “Exploring the progress and challenges of ultrasonic technology in environmental remediation,” *Ultrasonics Sonochemistry*, vol. 112, p. 107175, 2025, doi: 10.1016/j.ultsonch.2024.107175
[21] S. Zakeri, T. Vastamäki, M. Honkanen, M. Järveläinen, M. Vippola, and E. Levänen, “Fabrication of self-supporting structures made of washcoat materials (Gamma AL_2O_3-CeO_2) by ceramic stereolithography: Towards digital manufacturing of enhanced catalytic converters,” *Materials & Design*, vol. 210, p. 110115, 2021, doi: 10.1016/j.matdes.2021.110115
[22] I. Bieloshapka, P. Jiricek, Y. Yakovlev, K. Hruska, E. Tomsik, J. Houdkova, A. Malolepszy, M. Mazurkiewicz, Y. Lobko, and B. Lesiak, “Thermal and chemical activation methods applied to DFAFC anodes prepared by magnetron sputtering,” *International Journal of Hydrogen Energy*, vol. 45, no. 27, pp. 14133-14144, 2020, doi: 10.1016/j.ijhydene.2020.03.116
[23] E. Bonyadi, F. Z. Ashtiani, S. Ghorabi, and A. S. Niknejad, “Bio-inspired hybrid coating of microporous polyethersulfone membranes by one-step deposition of polydopamine embedded with amino-functionalized SiO_2 for high-efficiency oily wastewater treatment,” *Journal of Environmental Chemical Engineering*, vol. 10, no. 1, p. 107121, 2022, doi: 10.1016/j.jece.2021.107121
[24] D. Feriyanto, S. Sani Abdul Malik, M. Fitri, I. Hidayat, H. Pranoto, and S. Zakaria, ”Effect of Material Composition on Thermal Stability Analysis of Coated and Uncoated FeCrAl CATCO by γ-Al2O3 Ultrasonic-Electroplating Technique”, *Journal of Sustainable Materials Processing and Management*, vol 1, no.1, pp. 1-7, 2021, doi: 10.30880/jsmpm.2021.01.
[25] I. Hidayat, D. Feriyanto, H. Pranoto, Gian Villani Golwa, and Supaat Zakaria, ”Crystallite size and Solid Solubility Cr to Fe analysis of Fe80Cr20 Interconnect Material Treated by Ultrasonic and High Energy Ball milling Process,” *Res Militaris*, vol.12, no. 6, pp. 414-422, 2022.
[26] D. Feriyanto and S. Zakaria, ”New method of fabrication of Fe80Cr20 Alloy: Effect of its technique on crystallite size and thermal stability”, International Journal of Advanced Technology in Mechanical,” *Mechatronics and Materials*, vol. 1, no. 1, pp. 26-31, 2020, doi: 10.37869/ijatec.v1i1.11